

On the kinematic identification of the hurdles race using Cardan's rotation

MIHAI TOFAN, SORIN VLASE, HORATIU TEODORESCU
 Department of Mechanical Engineering
 Transilvania University of Braşov
 29 Eroilor Blvd., 500036 Braşov
 ROMANIA

Abstract: - In this paper the authors wish to make an adequate mathematical model to study some special motion of an athlete. Such motion has some particularities as the fact that there are great forces and great accelerations acting on different parts of the human body. A kinematical model, in order to identify the main motion of the parts of the body, is made. The mathematical used for dynamic analysis is strong non-linear and for this reason involve some difficulties in solving the problem. This need an adequate parameterization of human body and the identification of the best modality to introduces power in the system.

Key-Words: - Cardan's finite rotations, Kinematical analysis, Hurdles race, Biomechanical joints, Polynomial functions, Polynomial approximations, Vibe laws, Vibe burning acceleration.

1 Introduction

The study of the jump over barrier in hurdles begins from a sequence of 9 positions, shown in fig. 1, of which the angular positions α of the athlete's body and limbs with 9 segments were extracted, extended body with shoulders and hips, being built up by 9 articulated rods, body + 2 x 4 segments of limbs, fig. 2. Biomechanical joints:

Those belonging to the extended body are approximated with spherical joints, respectively cylindrical. Those internal of the limbs, respectively elbows and knees, are approximated with cylindrical joints. The biomechanical joints perform in reality small displacements and Kovacs W. [1] could classify them depending of contact surface and displacements, in 7 types of specific connections.

2 Matrix of positioning by Cardan rotations in spherical joints

Matrix of positioning by Cardan rotations in spherical joints. Lines 1,2 right leg - lead, line 3 / body, lines 4 - 7 left leg - trailed:

$$\alpha := \begin{pmatrix} -90 & -95 & -110 & -105 & -90 & -85 & -40 & -10 & 13 \\ 35 & -5 & -45 & -80 & -80 & -75 & -30 & -10 & 15 \\ 21 & 24 & 30 & 45 & 60 & 70 & 49 & 10 & 15 \\ 21 & 24 & 30 & 38 & -65 & -70 & -80 & -90 & -80 \\ 21 & 24 & 30 & 52 & 70 & 80 & 80 & 70 & -10 \\ 0 & 0 & 0 & 10 & 40 & 80 & 35 & 0 & 0 \\ -9 & -9 & 0 & 3 & 20 & 45 & 50 & 0 & 0 \end{pmatrix} \cdot \text{rd} \quad (1)$$

$$RB(f) = RZ(f_1) \cdot RX(f_2) \cdot RY(f_0), \quad (2)$$

$$h = 0 \dots M \quad j = 0 \dots m, \quad (3)$$

$$\delta 0^j = \{ \alpha_{3,j} \quad \alpha_{5,j} \quad \alpha_{6,j} \}^T, \quad (4)$$

$$\delta 1^j = \{ \alpha_{4,j} \quad \alpha_{5,j} \quad \alpha_{6,j} \}^T. \quad (5)$$

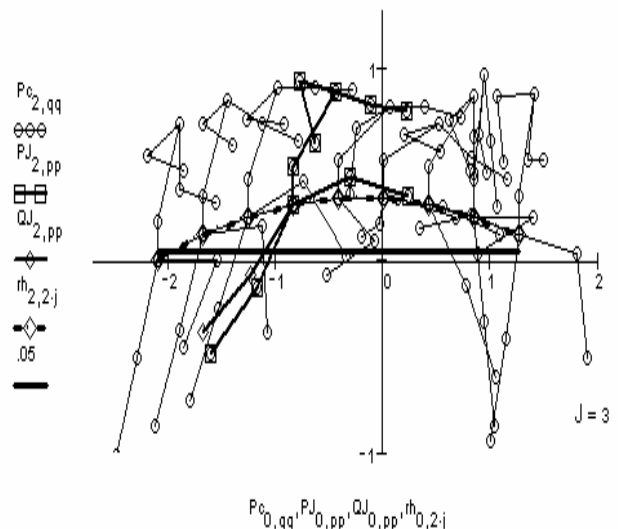


Fig. 1 The reference sequence [2] with 9 positions (J=3)

In the paper for positioning of the left leg were used modified Cardan rotations:

$$RB(f) = RZ(f_1) \cdot RX(f_2) \cdot RY(f_0), \quad (6)$$

but consequently – with analogue results - were used modified Euler rotations:

$$RE(f) = RY(f_1) \cdot RX(f_2) \cdot RY(f_0), \quad (7)$$

or:

$$RE(f) = RY(f_1) \cdot RZ(f_2) \cdot RY(f_0), \quad (8)$$

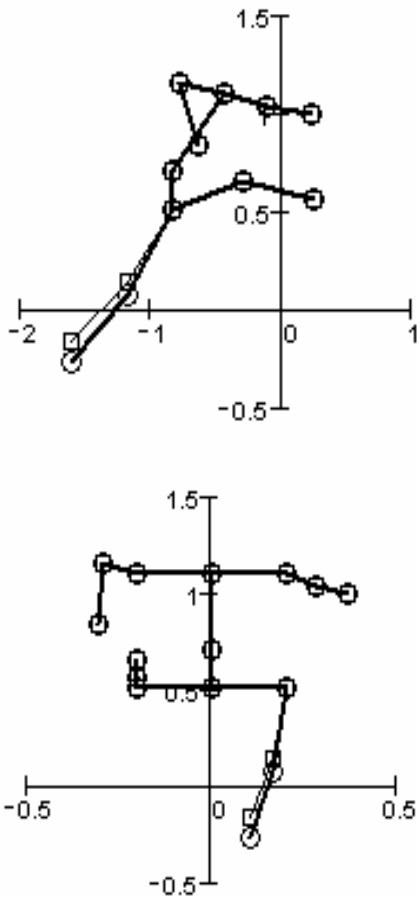


Fig. 2 Side view of the athlete, in sagittal plane and front plane (J=3)

The approximation of the matrix was made easily by polynomial functions, just for positioning of the leading leg, first two lines are shown in fig.3:

$$a0_h = -(M-h)^2 \cdot \left(\frac{h}{61.45}\right)^2 + \alpha_{0,0} \cdot \left(1 - \frac{h}{M}\right) + \alpha_{0,8} \cdot \frac{h}{M}, \quad (9)$$

$$a1_h = -(M-h)^2 \cdot \left(\frac{h}{44.9}\right)^2 + \alpha_{1,0} \cdot \left(1 - \frac{h}{M}\right) + \alpha_{1,8} \cdot \frac{h}{M}. \quad (10)$$

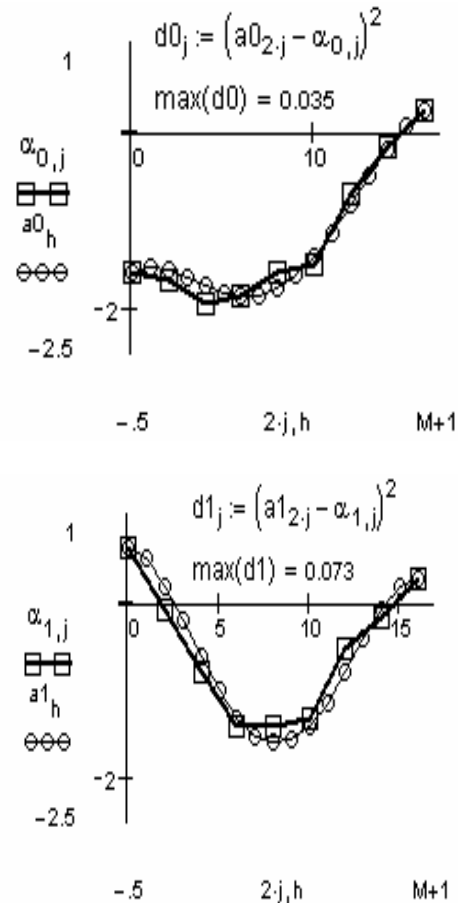


Fig. 3 The polynomial approximation of the first two lines, the angular positions of the right leg – leader.

The approximation of the next lines was made much easier, by two dual Vibe burning laws [3.4].

Vibe burning law applied on [0,1] interval:

$$C = \ln(10^3), \quad C = 6.908, \quad (11)$$

$$f(t,m) = 1 - e^{-C \cdot t^{m+1}}. \quad (12)$$

Vibe burning speed – derivative by t:

$$w(t,m) = C \cdot (m+1) \cdot t^m \cdot \exp(-C \cdot t^{m+1}). \quad (13)$$

Vibe burning acceleration:

$$W(t,m) = C \cdot (m+1) \cdot t^m \cdot \exp(-C \cdot t^{m+1}) \cdot \left(\frac{m}{t} - C \cdot (m+1) \cdot t^m\right). \quad (14)$$

So, for positioning of the body – shown in the third line it yields:

$$a2s_j = f\left(\frac{2 \cdot j}{M}, 2\right) \cdot (\alpha_{2,4} - \alpha_{2,0}) \cdot 1.5 + \alpha_{2,0}, \quad (15)$$

$$M = 16, \quad (16)$$

$$in = 0 \dots 3, \quad n = 0, 2 \dots 3, \quad (17)$$

$$k_{in,j} = (m+1) \cdot in + j, \tag{18}$$

$$\alpha_{2s}^j = \left(2j \quad a_{2s}^j \right)^T, \tag{19}$$

$$\alpha_{2d}^j = \left(2j \quad a_{2d}^j \right)^T, \tag{20}$$

$$ap_{in,j} = f\left(\frac{2j}{M}, \mathbf{m}_{in}\right) \cdot (\alpha_{2,7} - \alpha_{2,4}) - \alpha_{2,4}, \tag{21}$$

$$AP^{k_{in,j}} = \left(2j \quad ap_{k_{in,j}} \right)^T, \tag{22}$$

$$\mathbf{m}^T = (5 \quad 6 \quad 7 \quad 8), \tag{23}$$

$$a_{2d}^j = f\left(\frac{2 \cdot j}{M}, 7\right) \cdot (\alpha_{2,7} - \alpha_{2,4}) + \alpha_{2,4}, \tag{24}$$

$$m = 16, \tag{25}$$

$$k_{jn,j} = (m+1) \cdot jn + m - 1, \tag{26}$$

$$\mathbf{m} = 5 + in, \tag{27}$$

$$\varepsilon_{2j} = \text{if}(j < 4, \alpha_{2s}^j, \alpha_{2d}^j), \tag{28}$$

$$DV_{in} = m^{-1} \sum_j (ap_{k_{in,j}} - \alpha_{2,j})^2, \tag{29}$$

$$an = 0 \dots k_{3,m}, \tag{30}$$

$$DV^T = (.392 \quad .397 \quad .375 \quad .377), \tag{31}$$

$$a_{2d}^h := -f\left(\frac{h}{M}, 7.5\right) \cdot 1.17 + 1.33, \tag{33}$$

$$\alpha_{2h} := \text{if}(h < 9, a_{2s}^h, a_{2d}^h), \tag{34}$$

$$DV_0 := m^{-1} \cdot \sum_j (\alpha_{2_{2j}} - \alpha_{2,j})^2, \tag{35}$$

Root deviation:

$$DV = (3.545 \times 10^{-3}) \tag{36}$$

by this, becoming accessible the choose the most suitable kinetic integer exponent m, m = 7, which corresponds to the smallest root deviation, even with the naked eye, as in fig.3.

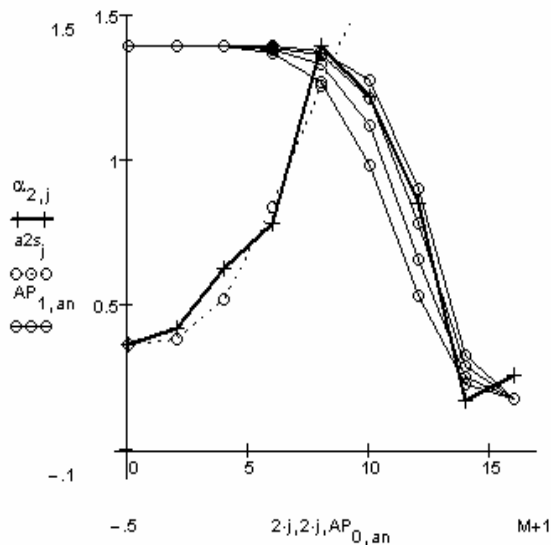


Fig. 4 Choosing the right approximate of the body motion

If fractional values of the kinetic exponent m are used, root deviation decrease even more:

$$a_{2s}^h := f\left(\frac{h}{M}, 1.8\right) \cdot 1.12 + \alpha_{2,0}, \tag{32}$$

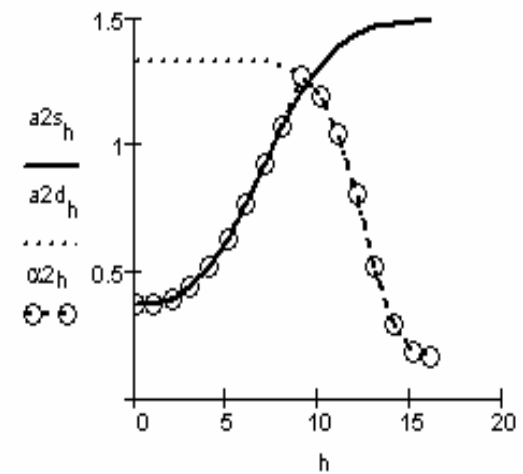
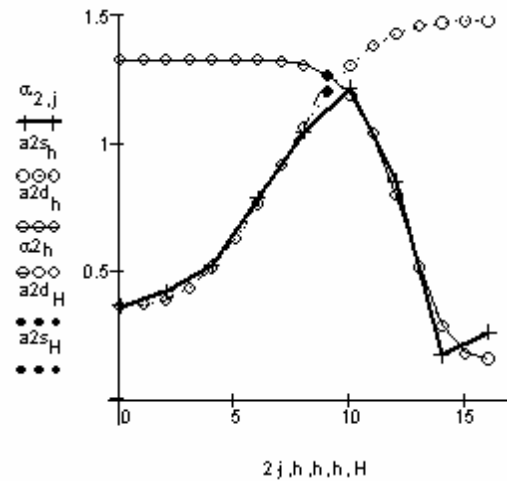


Fig. 5 The approximation of the body motion by Vibe laws of kinetics of oxidation reactions with kinetic fractional exponent, estimated with naked eye.

Angular velocity of the body is the speed of oxidation of the Vibe law of burning.

Studying the evolutions in fig 6, 7, the surprisingly fast evolution in this joint is to be pointed out. The shifting of the motion way is made extremely quickly.

This surprising finding is checked in every next joint, lines 4 ... 7, corresponding to the left – trailed – leg. The observation is general.

Vibe burning speed:

$$w(t,m) := C \cdot [t^m \cdot (m + 1)] \cdot \exp(-C \cdot t^{m+1}), \tag{37}$$

$$v2s_h := w\left(\frac{h}{M}, 1.8\right) \cdot 1.12, \tag{38}$$

$$\cdot w\left(\frac{h}{M}, 7.5\right) \cdot 1.17,$$

$$\omega2_h := \text{if}(h < 9, v2s_h, v2d_h). \tag{39}$$

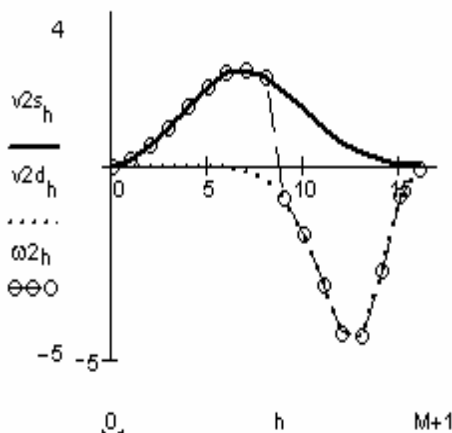


Fig. 6 Angular speed of the body

Vibe burning acceleration:

$$W(t,m) := C \cdot t^{m \cdot (m+1)} \cdot \exp[-C \cdot t^{(m+1)}] \cdot \left[\frac{m}{t} - C \cdot t^m \cdot (m+1) \right], \tag{40}$$

$$e2s_h := W\left(\frac{h}{M}, 1.8\right) \cdot 1.12, \tag{41}$$

$$e2d_h := -W\left(\frac{h}{M}, 7.5\right) \cdot 1.17, \tag{42}$$

$$e2_h := \text{if}(h < 9, e2s_h, e2d_h). \tag{43}$$

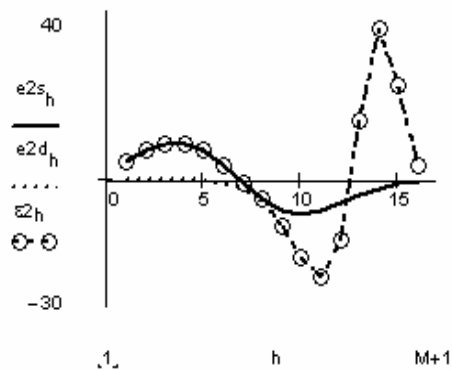


Fig. 7 Angular acceleration of the body. Concordant results.

this seems to be more natural to the movements of the sprinter.

3 Conclusions

Kinematics in biomechanical joint is way different of the pendulum movement in gravitational field, or technical joint, as shown in pictures in fig. 5 – 8. The shifting of the way of the speed in the biomechanical joint is much brutal.

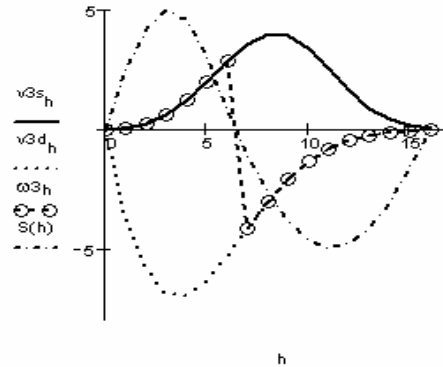


Fig. 8 The angular speed in biomechanical joint of the hip of the left-trailed-leg.

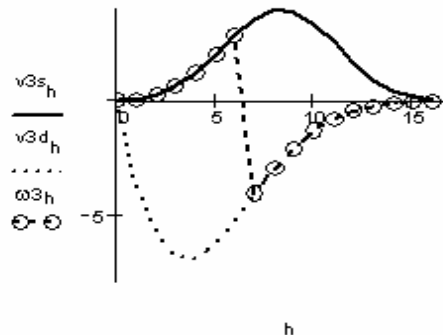


Fig. 9 Burning speed – the derivative of the burning law by t in the same hip joint of the left leg.

Now comes out the extension of the sequence from fig. 1 in Fig. 10 – 13.

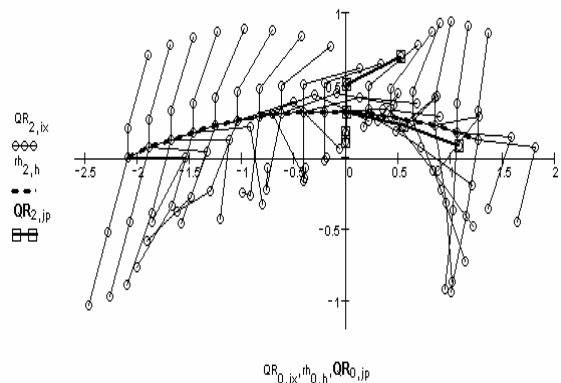


Fig. 10 Sequence extended by interpolation to 18=2x9 positions side view, in sagittal plane of the sprinter (H=10)

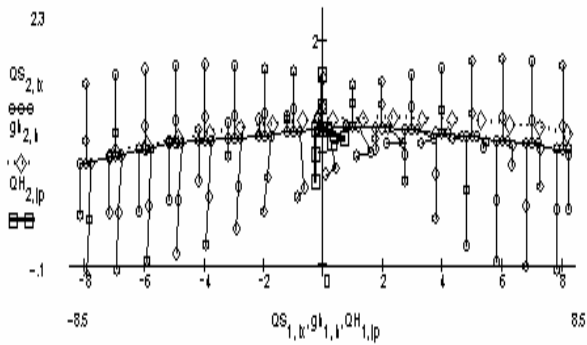


Fig. 11 Front view of the extended sequence.

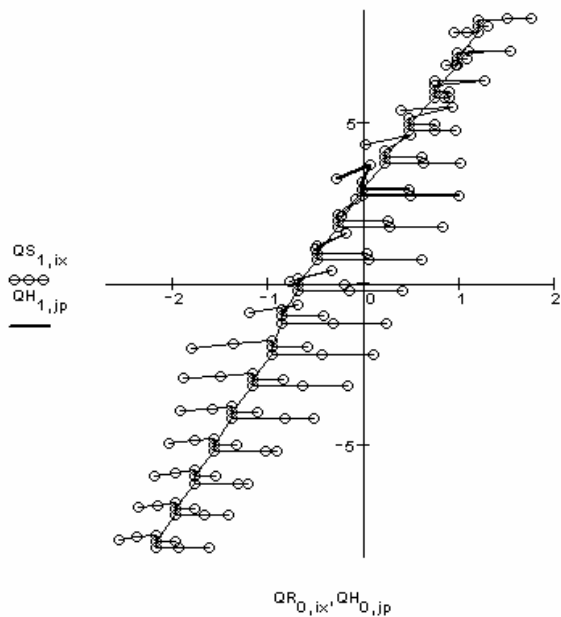


Fig. 12 Top view of the extended sequence.

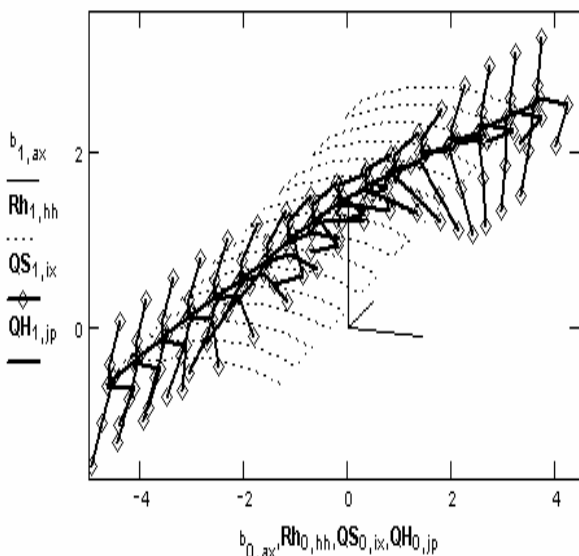


Fig. 13 3D view of the same sprinter on different lanes

extended body and the two legs – two segments each – the 5 rods model.

References:

- [1] Kovacs, W., *Biomechanical joints of the human limbs*, Timisoara, 1963 (in Romanian).
- [2] Burca, I., *Today evolution of the researches in analysis of the athletic motions*, Essay for M.D., Brasov, 2003 (in Romanian).
- [3] Vibe, I.I., *Brennverlauf und Kreisprozess von Verbrennungsmotoren*, VEB Verlag Technik, Berlin, 1970.
- [4] Tofan, M., Ulea, M., *Computer generating of the Otto/Diesel engine operating cycle*, *Buletinul Univ. Brasov*, Vol. XIX-B, 1977.
- [5] Tofan, M., *Kinematics*, Transilvania University of Brasov, 1981. (in Romanian).
- [6] Tofan, M., *Finite kinematics*, Transilvania University of Brasov, 1996. (in Romanian).

The extended sequences are built with a reduced model of the sprinter, without upper limbs, only the